

Synthesis, Spectroscopic and Magnetic Properties of Linear Nickel(II) and Cobalt(II) Trimers Containing Substituted 1,2,4-Triazoles and Fluoride as Bridging Ligands. The X-ray Structure of bis[(μ -fluoro)bis(μ -3,4,5-trimethyl-1,2,4-triazole- N^1,N^2)]bis(thiocyanato- N)(aqua)cobalt(II)- F,N^1,N^1'] cobalt(II) Tetrahydrate

FREDERIK J. RIETMEIJER, JAAP G. HAASNOOT, ADRIANUS J. DEN HARTOG and JAN REEDIJK*

Department of Chemistry, Gorlaeus Laboratories, State University Leiden, 2300 RA Leiden, The Netherlands

Received August 16, 1985

Abstract

The preparation and properties of a new series of triazole- and fluoro-bridged trimeric compounds, containing Co(II) and Ni(II) as metal ions, are described. The compounds have the general formula $M_3L_4F_2(NCS)_4(H_2O)_x$, where L denotes 3,5-dimethyl-1,2,4-triazole (dmtrH, $C_4H_7N_3$), 4-amino-3,5-dimethyl-1,2,4-triazole (admtr, $C_4H_8N_4$), 3,4,5-trimethyl-1,2,4-triazole (tmtr, $C_5H_9N_3$) and 4-amino-3,5-diethyl-1,2,4-triazole (adetr, $C_6H_{12}N_4$), respectively, and $x = 2-6$. Dark red crystals of $[Co_3(tmtr)_4F_2(NCS)_4(H_2O)_2](H_2O)_4$ are monoclinic, space group $P2_1/n$, with $a = 9.834(2)$, $b = 12.106(1)$, $c = 18.657(2)$ Å, $\beta = 99.60(1)^\circ$, $V = 2190$ Å³ and $Z = 2$; the measured and calculated densities are 1.52(1) and 1.52 Mg m⁻³, respectively. The X-ray analysis was done using counter data (3642 significant reflections). The structure was solved by the heavy atom method and refined by full-matrix least-squares methods to a final R of 0.034 ($R_w = 0.045$). Neighbouring Co(II) ions in the linear trimer are linked by two 1,2-bidentate triazole ligands and one fluoride anion. The coordination sphere of the terminal Co(II) ions is completed by two N-bonded thiocyanate anions and one water molecule. The Co...Co distance in the trimer is 3.4015(3) Å. The Co-F distances are 2.023(1) and 2.058(2) Å, whereas the Co-N(triazole) distances are somewhat larger (2.13–2.17 Å). The magnetic properties of the trimeric Ni compounds are satisfactorily described by the isotropic Heisenberg model, yielding characteristic exchange constants J in the range -11 – -15 cm⁻¹ and g -factors in the range 2.20–2.27. An Ising type of Hamiltonian is used for the interpretation of the magnetic data of the cobalt trimers, assuming an effective spin of 1/2 for Co and neglecting χ_L . The exchange constants J_{\parallel} obtained range from -7 to -35 cm⁻¹ with g_{\parallel} values of 6.1–9.2. These values are rough estimates only, because the good agreement

with theory only occurs at temperatures below 20 K. The magnetic properties of the compounds are compared to magnetic data of closely related compounds.

Introduction

Recent structural and magnetic studies of fluoride-bridged coordination compounds are aimed at rationalizing the sign and magnitude of the exchange constant J in terms of structural features, such as the M–F–M bridging angle [1–5]. For hydroxo-, azido-, chloride- and bromide-bridged compounds, such studies are well known [6–13]. Fluoride-bridged transition-metal complexes, however, are not well documented because of their tedious preparation. Recently it was found [14] that linear trinuclear compounds are formed when transition-metal (Co, Mn, Ni) thiocyanates are allowed to react with 3,5-dialkyl-1,2,4-triazoles; the resulting species contain two 1,2-bidentate triazoles and one N-coordinated thiocyanate anion as bridging framework. In a similar reaction, mixtures of transition-metal thiocyanates and fluorides (tetrafluoroborates may be used also as a source of fluoride) yield trimeric compounds in which the metal ions are linked by two 1,2-bidentate triazole ligands and one fluoride anion; this is illustrated by the crystal structure of $[Co_3(dettrH)_6F_2(NCS)_4](H_2O)_2$ (dettrH = 3,5-diethyl-1,2,4-triazole) [4].

We now report a series of linear Co- and Ni-trimers containing a similar fluoride- and triazole bridging framework; the general formula $M_3L_4F_2(NCS)_4(H_2O)_x$ (L = substituted triazole, $x = 2-6$) suggests that water might be present in the coordination sphere of the terminal Co ions, and this is illustrated by the crystal structure of a representative compound. The spectroscopic and magnetic properties of the eight compounds are discussed, and compared to structural and magnetic data of related compounds.

*Author to whom correspondence should be addressed.

Experimental

Starting Materials

Co(II) and Ni(II) thiocyanate were freshly prepared or generated *in situ* from commercially available metal(II) nitrates and ammonium thiocyanate. Both commercially available metal(II) fluorides (M = Co, Ni) and metal(II) tetrafluoroborates (used as aqueous solutions) can be used as a source of fluoride anions [1, 4]. The ligand 3,4,5-trimethyl-1,2,4-triazole was prepared by reaction of 2,5-dimethyl-1,3,4-oxadiazole (synthesized by dehydration of sym. diacetylhydrazine with P₂O₅ [15]) with methylamine according to Duffin [16]. The syntheses of the other ligands used have been described earlier [14].

Syntheses of the Coordination Compounds

The trimeric clusters were synthesized by reaction of the ligand with CoF₂ and NiF₂·4H₂O, respectively, followed by the addition of metal(II) thiocyanate solution. 2.5 mmol of CoF₂ or NiF₂·4H₂O and 5.0 mmol of the ligand L (L = admtr, adetr, dmtrH, tmtr) were dissolved in 25 ml of boiling water; the solution was filtered to remove any insoluble material and a solution of the metal(II) thiocyanate (2.5 mmol in 25 ml of water) was added slowly. In all cases, compounds having the general formula M₃L₄F₂(NCS)₄(H₂O)_x crystallized rapidly (L = admtr, x = 4; L = adetr, x = 2; L = dmtrH, tmtr, x = 6). Changing the ratio MF₂:M(NCS)₂:L to 1:2:2 resulted in products with nearly identical IR spectra and X-ray powder patterns, although a trace of end-on isothiocyanato-bridged product (characteristic ν_{CN} stretching in the IR at 2000 cm⁻¹) could be detected in the latter compounds. The alternative synthetic procedure mentioned above, involving decomposition of the BF₄⁻ anion, is as follows: 2.5 mmol of metal(II) tetrafluoroborate (M = Co, Ni) and 2.5 mmol of metal(II) thiocyanate were dissolved in 25 ml of hot water, the solution was filtered and the ligand solution (5.0 mmol in 10 ml of water) was added slowly. Crystallization occurred on standing at room temperature.

Physical and Analytical Measurements

Metal analyses were performed using standard EDTA titration techniques. C, H, N, S and F analyses were carried out by the Microanalytical Laboratory of the University College, Dublin, Ireland, and the Microanalytical Laboratory of Dr. Pascher, Bonn, F.R.G. Infrared spectra were obtained as nujol mulls and KBr pellets (4000–200 cm⁻¹) on a Perkin-Elmer 580B spectrophotometer. Ligand field spectra were obtained by the diffuse-reflectance method on the solid powders. Magnetic susceptibility measurements down to 4 K were carried out at the Centre d'Etudes Nucléaires de Grenoble, France, at the Department

of Chemistry of the University of New Orleans, U.S.A., and in our own laboratory, using a PAR vibrating sample magnetometer equipped with a Janis-type cryostat.

X-ray Data Collection and Refinement

Crystallographic data and relevant information on the data collection and refinement have been summarized in Table I. A nearly cubic crystal of approximate dimensions 0.30 mm × 0.30 mm × 0.25 mm was mounted and used for the data collection. Intensity data were collected in ω–θ scan mode for all reflections with 2° < θ < 30° and with k > 0 and l > 0, using graphite-monochromized Mo Kα radiation (λ = 0.7107 Å). The mosaic spread of the crystal was less than 0.35°. Diffractometer data were indicative of the monoclinic space group P2₁/n (systematic absences h0l if h + l ≠ 2n, 0k0 if k ≠ 2n). The scanning rate was adjusted to the required precision of σ(I) < 0.01 I, with a maximum scan time of 60 s per reflection. Intensities I and their estimated standard deviations were calculated from counting statistics. Three standard reflections were measured after every 5400 s of radiation time to check for instrumental instability and crystal decomposition; during the data collection there was a 6% decrease in intensity, for which the data were corrected. Lorentz and polarization corrections were applied. The maximal variation in the intensity of three suitable reflections at different azimuthal positions (see the transmission range in Table I), the crystal habit and the value of μ suggested that correction for absorption was unnecessary. Examination of observed and calculated structure factors led to the conclusion that extinction effects were negligible. Scattering factors, including anomalous dispersion, were taken from ref. 17. The cobalt positions, located in a Patterson synthesis, were used as input data for AUTOFOUR, a program for automatic crystal structure determination developed in our laboratory [18]. Nearly all non-hydrogen atomic positions were obtained in this way. The remaining atoms could be located by subsequent least-squares refinement cycles followed by difference Fourier syntheses. The refinement was carried out using weights 1/σ²(F), with σ(F) = σ(F) counting statistics + 0.03 F. The positional and thermal parameters of the hydrogen atoms located were not refined; the B_{iso} values were fixed at the initial B_{iso} value of the corresponding mother atom. A few hydrogen atom positions were calculated. The final difference Fourier synthesis showed a few residual peaks near the oxygen atom O(2) of a water molecule (probable disorder) and near the thiocyanate sulfur atom S(1); the latter fact and the high thermal anisotropy of sulfur atom S(2) indicate that both sulfur atoms are probably slightly disordered. The final values of the residuals were R = 0.034, R_w = 0.045 for

TABLE I. Crystal and Diffraction Data of $[\text{Co}_3(\text{tmtr})_4\text{F}_2(\text{NCS})_4(\text{H}_2\text{O})_2](\text{H}_2\text{O})_4$

Crystal color	dark red
Crystal shape	nearly cubic
M_w (g mol ⁻¹)	999.8
Space group	$P2_1/n$
a (Å)	9.834(2)
b (Å)	12.106(1)
c (Å)	18.657(2)
β (deg)	99.60(1)
V (Å ³)	2190
Z	2 (trimers)
D_{meas}^a (Mg m ⁻³)	1.52(1)
D_{calc} (Mg m ⁻³)	1.52
$F(000)$	1024.8
θ range (deg)	2–30
Octants collected	$k > 0, l > 0$
Measured reflections	6831
Independent reflections	6648
Significant reflections ($I > 2\sigma(I)$)	3642
Agreement factor between equivalent reflections	0.026
T , data collection	Room temperature
Radiation used ^b	Mo K α ($\lambda = 0.7107$ Å)
Diffraction type	Enraf-Nonius CAD-4
μ (cm ⁻¹)	13.7
Final R -value ($(\sum F_o - F_c)/\sum F_o $)	0.032
Final R_w -value ($(\sum w(F_o - F_c)^2/\sum w F_o ^2)^{1/2}$)	0.043
Transmission range (azimuth scan)	0.92–1.06

^aMeasured by flotation in $\text{CHCl}_3/\text{C}_2\text{H}_4\text{Br}_2$. ^bGraphite-monochromized.

TABLE II. Fractional Atomic Coordinates ($\times 10^5$ for Co, $\times 10^4$ for the other atoms) and Equivalent Isotropic Thermal Parameters ($\times 10^3$ for Co, $\times 10^2$ for the other atoms) in $[\text{Co}_3(\text{tmtr})_4\text{F}_2(\text{NCS})_4(\text{H}_2\text{O})_2](\text{H}_2\text{O})_4$ ^a

Atom	x/a	y/b	z/c	B_{iso}
Co(1)*	0	0	0	2272(12)
Co(2)	21454(4)	17794(3)	10532(2)	2805(9)
N(1)	3956(3)	2705(2)	1176(1)	397(7)
C(1)	4895(3)	3273(3)	1345(2)	362(8)
S(1)	6201(1)	4091(1)	1571(1)	632(3)**
N(2)	2466(3)	1264(2)	2129(1)	424(7)
C(2)	2411(3)	1029(2)	2716(2)	352(7)
S(2)	2373(1)	709(1)	3557(1)	598(3)
F	323(2)	909(1)	922(1)	275(3)
O	1068(3)	3239(2)	1346(1)	468(7)
N(11)	2116(2)	-453(2)	274(1)	274(5)
N(12)	3015(2)	265(2)	700(1)	295(6)
C(13)	4178(3)	-251(3)	871(2)	334(8)
N(14)	4083(2)	-1273(2)	584(1)	342(6)
C(15)	2776(3)	-1375(2)	211(1)	306(7)
C(C13)	5469(3)	184(3)	1333(2)	488(10)
C(N14)	5157(4)	-2138(3)	654(2)	525(11)
C(C15)	2214(3)	-2368(3)	-197(2)	415(9)
N(21)	608(2)	1481(2)	-501(1)	266(5)
N(22)	1452(2)	2229(2)	-73(1)	272(6)
C(23)	1608(3)	3085(2)	-482(2)	301(7)
N(24)	904(2)	2908(2)	-1162(1)	300(6)
C(25)	280(3)	1914(2)	-1152(1)	284(6)
C(C23)	2358(4)	4118(3)	-250(2)	441(9)

TABLE II (continued)

Atom	x/a	y/b	z/c	B_{iso}
C(N24)	906(4)	3632(3)	-1789(2)	480(9)
C(C25)	-684(3)	1450(3)	-1764(2)	389(8)
O(1)	-1252(3)	900(2)	2012(1)	588(8)
O(2)	-765(4)	3053(3)	2326(2)	940(13)

^aEstimated standard deviations in the least significant digits are given in parentheses. The atoms marked** show high thermal anisotropy. Special positions are marked*.

3642 significant reflections. Atomic positions and equivalent isotropic thermal parameters of the non-hydrogen atoms are listed in Table II. Listings of observed and calculated structure factors, hydrogen atom positions, and the anisotropic thermal parameters of the non-hydrogen atoms are available, see 'Supplementary Material'.

Results and Discussion

General

Table III contains the X-ray powder-patterns, ligand field data and characteristic IR data of the eight compounds reported. The results of elemental analyses (metal, C, H, N, F, S) are satisfactory and

TABLE III. Trimeric Coordination Compounds $M_3L_4F_2(NCS)_4(H_2O)_x$ ($M = Ni, Co; x = 2-6$) with X-ray Powder Isomorphism, Ligand Field Data and Characteristic IR Data; sh = shoulder, b = broad

Formula	X-ray powder type	ν_{CN} (cm^{-1})	M-F (cm^{-1})	Ligand field maxima (kK)	Dq (cm^{-1})	B (cm^{-1})
$Ni_3(dmtrH)_4F_2(NCS)_4(H_2O)_6$	A	2135,2100	380,355	9.4,12.9(sh),15.7,21.5(sh), 25.6	940	845
$Co_3(dmtrH)_4F_2(NCS)_4(H_2O)_6$	A	2120,2090,2060(sh)	370,340	8.7,16.0(sh),18.7	950	740
$Ni_3(tmtr)_4F_2(NCS)_4(H_2O)_6$	B	2110(sh),2100,2060(sh)	385,350	9.5,13.8(sh),16.1,26.7	950	920
$Co_3(tmtr)_4F_2(NCS)_4(H_2O)_6$	B	2100(sh),2090,2050(sh)	375,330	8.7,16.1(sh),20.0	950	830
$Ni_3(admtr)_4F_2(NCS)_4(H_2O)_4$	C	2110(b),2060(sh)	385,350	9.5,13.8(sh),16.1,26.7	950	920
$Co_3(admtr)_4F_2(NCS)_4(H_2O)_4$	C	2100(b),2050(sh)	375,335	8.9,16.1(sh),19.6,20.8(sh)	970	785
$Ni_3(adetr)_4F_2(NCS)_4(H_2O)_2$	D	2130,2100	395,345(b)	9.1,12.9(sh),15.7,25.6	910	885
$Co_3(adetr)_4F_2(NCS)_4(H_2O)_2$	D	2120,2080,2040(sh)	390,330(b)	8.7,18.2,19.6(sh),21.3(sh)	950	700

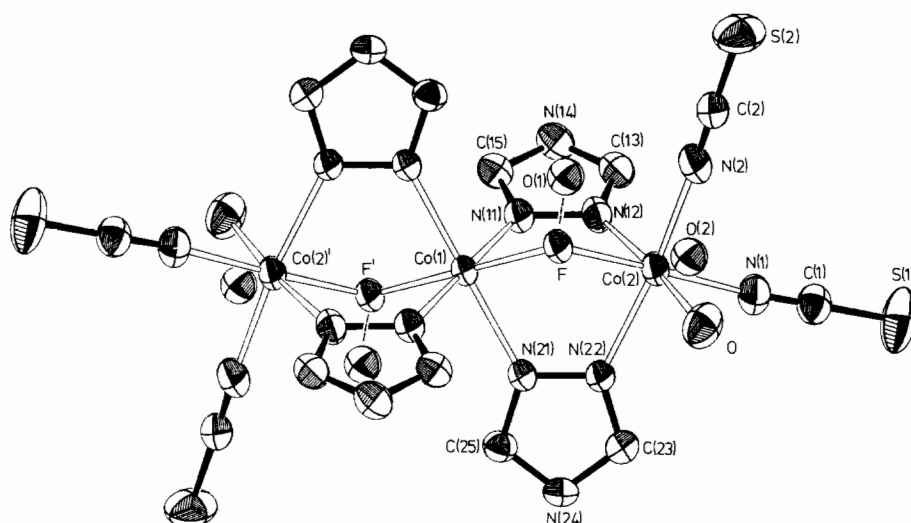


Fig. 1. ORTEP drawing of $[Co_3(tmtr)_4F_2(NCS)_4(H_2O)_2](H_2O)_4$, showing the atomic labeling scheme and the positions of the water molecules. The dotted lines indicate hydrogen bonds. Hydrogen bonding between O(1) and O(2) and between O and O(2) is not indicated in the figure. Primed atoms are generated by the centre of symmetry. Methyl groups of triazole ligands have been omitted for clarity. The numbering of the methyl groups, as mentioned in Table II, is as follows: C(Cn3), C(Nn4) and C(Cn5) are attached to C(n3), C(n4) and C(n5), respectively, where n denotes the number of the ring.

are available, see 'Supplementary Material'. The synthetic procedures described above are not successful in case of $M = Cu$. For a given ligand L, the infrared spectra and X-ray powder patterns of the Co and Ni trimers are similar. No isomorphism, however, is observed between compounds containing different ligands.

Molecular Structure of $[Co_3(tmtr)_4F_2(NCS)_4(H_2O)_2](H_2O)_4$

The centrosymmetric trimeric unit is shown in Fig. 1, together with the atomic labeling scheme used. Relevant bond lengths and angles are listed in Table IV. Bond distances and angles of the triazole rings are available, see 'Supplementary Material'.

Neighbouring Co(II) ions in the trimeric unit are linked by two bridging triazole ligands and one

fluoride anion. The octahedron of the central Co(II) ion is compressed along the F-Co-F' axis, given the distances $Co(1)-F = 2.023(1)$ Å, $Co(1)-N(11) = 2.131(2)$ Å and $Co(1)-N(21) = 2.152(2)$ Å. Two thiocyanate anions and one water molecule complete the coordination sphere of the terminal Co(II) ions; the $Co(2)-NCS$ distances of 2.084(3) and 2.075(3) Å, respectively, are essentially smaller than the $Co(2)-N$ (triazole) and $Co(2)-O$ (water) distances ($Co(2)-N(12) = 2.172(2)$ Å, $Co(2)-N(22) = 2.168(2)$ Å, and $Co(2)-O = 2.177(2)$ Å). These distances and the ligand-Co(2)-ligand angles are indicative of a distortion of the octahedron around Co(2). The terminal thiocyanate anions are coordinated in an almost linear fashion, as is indicated by the angles $Co(2)-N(1)-C(1) = 169.1(3)^\circ$ and $Co(2)-N(2)-C(2) = 168.3(3)^\circ$. The bridging angle $Co(1)-$

TABLE IV. Relevant Bond Lengths (Å) and Bond Angles (deg) in $[\text{Co}_3(\text{tmtr})_4\text{F}_2(\text{NCS})_4(\text{H}_2\text{O})_2](\text{H}_2\text{O})_4^{\text{a}}$. Primed atoms are generated by the symmetry operation $-x, -y, -z$

Co(1)···Co(2)	3.4015(3)	Co(1)–N(11)	2.131(2)
Co(1)–F	2.023(1)	Co(1)–N(21)	2.152(2)
Co(2)–F	2.058(2)	Co(2)–N(12)	2.172(2)
Co(2)–N(1)	2.084(3)	Co(2)–N(22)	2.168(2)
Co(2)–N(2)	2.075(3)	Co(2)–O	2.177(2)
N(1)–C(1)	1.152(4)	N(2)–C(2)	1.142(4)
C(1)–S(1)	1.621(3)	C(2)–S(2)	1.621(3)
Co(1)–F–Co(2)	112.92(7)	Co(2)–N(12)–N(11)	117.2(2)
Co(1)–N(11)–N(12)	118.6(2)	Co(2)–N(22)–N(21)	117.1(2)
Co(1)–N(21)–N(22)	118.5(2)		
Co(2)–N(1)–C(1)	169.1(3)	Co(2)–N(2)–C(2)	168.3(3)
F–Co(1)–N(11)	85.83(7)	F–Co(1)–N(11)′	94.17(7)
F–Co(1)–N(21)	84.32(7)	F–Co(1)–N(21)′	95.68(7)
F–Co(2)–N(12)	84.88(7)	F–Co(2)–N(22)	83.49(7)
N(11)–Co(1)–N(21)	89.32(8)	N(11)–Co(1)–N(21)	90.68(8)

^aEstimated standard deviations are given in parentheses.

TABLE V. Hydrogen Bond Distances (Å) and Angles (deg) in $[\text{Co}_3(\text{tmtr})_4\text{F}_2(\text{NCS})_4(\text{H}_2\text{O})_2](\text{H}_2\text{O})_4^{\text{a}}$

O···O(2)	2.783(4)	O–H(10)···O(2)	163.1(2)
O(1)···F	2.753(3)	O(1)–H(2O1)···F	163.8(2)
O(1)···O(2)	2.696(5)	S(1)···O(2)′	3.327(4)
S(2)···O″	3.351(2)	S(2)···H(2O)″–O″	172.1(2)
O(1)···S(1)″	3.428(3)	O(1)–H(1O1)···S(1)″	147.4(1)

^aEstimated standard deviations are given in parentheses. Single primes indicate the symmetry operation $1+x, y, z$; double primes indicate the symmetry operation $1/2-x, -1/2+y, 1/2-z$.

F–Co(2) = 112.92(7)°. The Co···Co distance in the trimer is 3.4015(3) Å. Hydrogen-bond distances and angles are given in Table V. Oxygen atom O(1), belonging to a non-coordinating water molecule is strongly hydrogen-bonded to the bridging fluoride anion (O(1)···F = 2.753(3) Å) and to the oxygen atom O(2) of another water molecule (O(1)···O(2) = 2.696(5) Å). An intramolecular hydrogen bond also exists between O(2) and the oxygen atom of the coordinated water molecule (O(1)···O(2) = 2.783(4) Å). From Table V it is clear that intermolecular hydrogen-bonding is weaker. One of the thiocyanate sulfur atoms is involved in a weak hydrogen bonding contact with a water molecule of a neighbouring trimer (S(1)···O(2)′ = 3.327(4) Å); sulfur atom S(2) is weakly hydrogen-bonded to a water molecule of another trimer (S(2)–O″ = 3.351(2) Å), whereas the distance O(1)–S(1)″ indicates a weak intermolecular contact between a water molecule and a thiocyanate sulfur.

A closely related X-ray structure published recently [4] is redrawn in Fig. 2. The formula of the compound is $[\text{Co}_3(\text{detrH})_6\text{F}_2(\text{NCS})_4](\text{H}_2\text{O})_2$, where

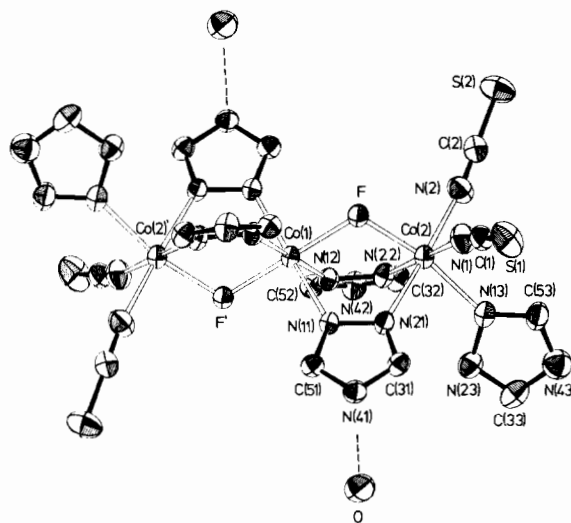


Fig. 2. ORTEP drawing of $[\text{Co}_3(\text{detrH})_6\text{F}_2(\text{NCS})_4](\text{H}_2\text{O})_2$, showing the atomic labeling scheme and the positions of the water molecules relative to the ligands. Primed atoms are generated by the centre of symmetry. Ethyl groups of triazole ligands have been omitted. The dotted lines represent hydrogen bonds.

detrH indicates 3,5-diethyl-1,2,4-triazole. The Co–F and the Co···Co distances are slightly shorter than in the structure reported here (Co–F distances 2.019(1) and 1.992(1) Å, respectively; Co···Co = 3.3726(3) Å). However, the Co(1)–F–Co(2) angle is larger (114.44(7)°). These structural features may be explained by the fact that the Co(2)–N(triazole) distances in $[\text{Co}_3(\text{detrH})_6\text{F}_2(\text{NCS})_4](\text{H}_2\text{O})_2$ are essentially larger (Co(2)–N distances 2.181(2) and 2.206(2) Å, respectively), resulting in a more asymmetric bridging framework. Another important

TABLE VI. Magnetic Susceptibility Data^a of $M_3L_4F_2(NCS)_4(H_2O)_x$ and $M_3(det\text{rH})_6F_2(NCS)_4(H_2O)_2$ ($M = \text{Ni, Co}$)

Compound	g	J (cm^{-1})	$\mu_{\text{eff}}^{80\text{K}}$ (BM)	θ (K) ^e
$\text{Ni}_3(\text{dmtrH})_4\text{F}_2(\text{NCS})_4(\text{H}_2\text{O})_6$	2.27(1)	-11.0(4)	2.63(5)	-61(2)
$\text{Co}_3(\text{dmtrH})_4\text{F}_2(\text{NCS})_4(\text{H}_2\text{O})_6$	7.5(1)	-13(1)	4.11(5)	-69(2)
$\text{Ni}_3(\text{tmtr})_4\text{F}_2(\text{NCS})_4(\text{H}_2\text{O})_6$	2.25(1)	-12.2(2)	2.57(5)	-56(2)
$\text{Co}_3(\text{tmtr})_4\text{F}_2(\text{NCS})_4(\text{H}_2\text{O})_6$	6.1(1)	-7(1)	4.00(5)	-64(2)
$\text{Ni}_3(\text{admtr})_4\text{F}_2(\text{NCS})_4(\text{H}_2\text{O})_4$	2.25(1)	-15(2)	2.45(5)	-79(2)
$\text{Co}_3(\text{admtr})_4\text{F}_2(\text{NCS})_4(\text{H}_2\text{O})_4$	7.64(9)	-17(1)	3.88(5)	-84(2)
$\text{Ni}_3(\text{adetr})_4\text{F}_2(\text{NCS})_4(\text{H}_2\text{O})_2$	2.20(1) ^c	-12.5(3) ^c	2.46(5) ^c	-69(2) ^c
$\text{Co}_3(\text{adetr})_4\text{F}_2(\text{NCS})_4(\text{H}_2\text{O})_2$	9.21(2) ^d	-34.7(5) ^d	3.80(5) ^d	-71(2) ^d
$\text{Ni}_3(\text{detrH})_6\text{F}_2(\text{NCS})_4(\text{H}_2\text{O})_2$	2.28(1) ^b	-11.1(9) ^b	2.70(5) ^b	-55(2) ^b
$\text{Co}_3(\text{detrH})_6\text{F}_2(\text{NCS})_4(\text{H}_2\text{O})_2$	8.23(4) ^b	-17.4(7) ^b	4.01(5) ^b	-67(2) ^b

^aThe data of the Ni trimers correspond to the Heisenberg model ($S = 1$). The Co trimers were fitted to the Ising model ($S' = 1/2$, $T < 80$ K). ^bThe data are taken from ref. 4. ^cOnly data with $T > 26$ K were taken into account; see text. ^dOnly data with $T > 16$ K were taken into account; see text. ^eDetermined by extrapolation of the high-temperature slope of $1/\chi$ vs. T .

difference between the two structures exists in the hydrogen-bonding pattern; in $[\text{Co}_3(\text{detrH})_6\text{F}_2(\text{NCS})_4](\text{H}_2\text{O})_2$, the bridging fluoride anion is not involved in hydrogen bonding contacts; in contrast, in $[\text{Co}_3(\text{tmtr})_4\text{F}_2(\text{NCS})_4(\text{H}_2\text{O})_2](\text{H}_2\text{O})_4$, the bridging fluoride anion is strongly hydrogen bonded to an uncoordinated water molecule.

Spectroscopic and Magnetic Properties

In Table III, the ligand field maxima and mean Dq and B values (calculated according to Reedijk *et al.* [19, 20]) of the Co and Ni trimers are listed. The rule of the average environment predicts that the Dq values of the central and terminal metal ions will be about equal. The observed maxima are in agreement with an octahedral environment for the metal ions [19, 20]. The observed Dq values are significantly lower than those observed for trimeric compounds containing triple triazole bridges [21, 22], as is to be expected in view of the position of fluoride anion in the spectrochemical series. For the Co trimers, the splittings of σ_3 (in most cases not well-resolved) probably arise from octahedral distortions. All Co-trimers turn blue or purple on heating or powdering thoroughly. The broadening of the absorption maxima observed suggests that tetrahedral Co species are formed.

Characteristic features of the IR spectra are the ν_{CN} stretchings of the terminal N-bonded thiocyanate anions and the M-F stretching vibrations. The ν_{CN} stretchings in the 2050–2130 cm^{-1} region [23–26] are observed as a doublet because of the mutual *cis* geometry of the thiocyanate anions. In several cases, this doublet is centered slightly above 2100 cm^{-1} , which is remarkable because this frequency region is usually restricted to thiocyanate anions bridging via the nitrogen and the sulfur atom (end to end) [27–29]. However, an extensive survey of the IR data of transition-metal thiocyanate com-

plexes [27] shows that the position of the ν_{CN} band alone as a criterion of bonding mode must be considered risky; many factors are involved and several examples are known of compounds disobeying this rule [30, 31]. In the 300–400 cm^{-1} region at least two absorptions are found that can be assigned to M-F vibrations; the frequencies observed are close to the values observed for $M_3(\text{detrH})_6\text{F}_2(\text{NCS})_4(\text{H}_2\text{O})_2$ and for $M\text{F}_2(\text{dmpz})_2$ chain compounds ($M = \text{Co, Ni}$; $\text{dmpz} = 3,5\text{-dimethylpyrazole}$) [1, 4]. The Irving-Williams sequence is obeyed. M-O stretching vibrations can not be located; these absorptions are probably weak and broadened because of hydrogen bonding. In all compounds, the δ_{NCS} bending vibrations are observed at 470 ± 5 cm^{-1} , whereas the ν_{CS} stretchings are found in the 780–790 cm^{-1} region [32, 33].

All compounds were also studied by magnetic susceptibility measurements down to 4 K. Results are given in Table VI. For comparison, magnetic data of $[M_3(\text{detrH})_6\text{F}_2(\text{NCS})_4](\text{H}_2\text{O})_2$ ($M = \text{Co, Ni}$) are included [4]. Several reports dealing with the magnetic behaviour of Ni trimers are known from the literature [34–38]. The magnetic exchange interactions in centrosymmetric trimers can be described by the isotropic Hamiltonian $\mathcal{H} = -2J \cdot [(S_1 \cdot S_2) + (S_2 \cdot S_3)] - 2J_{13}(S_1 \cdot S_3)$, where J and J_{13} represent the exchange constants between neighbouring and terminal metal ions, respectively. In the absence of a clearly defined exchange pathway between the terminal metal ions, J_{13} was taken as zero [14, 35, 37]. Furthermore, the spectroscopic splitting constant g was assumed to be identical for all the individual ions, and zero-field splittings and intercluster interactions were neglected. Contributions of diamagnetic susceptibility and temperature-independent paramagnetism were introduced as minor corrections to χ . The function minimized in the least-squares fitting procedure was $\Sigma(\chi_{\text{obs}}^i -$

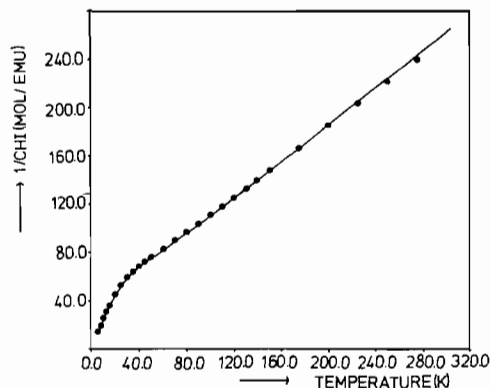


Fig. 3. Plot of the reciprocal magnetic susceptibility ($1/\chi$) vs. temperature of $[\text{Ni}_3(\text{tmtr})_4\text{F}_2(\text{NCS})_4(\text{H}_2\text{O})_2](\text{H}_2\text{O})_4$. The drawn curve is the theoretical prediction of a linear $S=1$ Heisenberg trimer with $g=2.25(1)$ and $J=-12.2(2)$ cm^{-1} (diamagnetic correction = -175×10^{-6} e.m.u., T.I.P. = 200×10^{-6} e.m.u. per Ni).

χ_{calc}^{-1})². The $1/\chi$ vs. T plot of $\text{Ni}_3(\text{tmtr})_4\text{F}_2(\text{NCS})_4(\text{H}_2\text{O})_6$ is shown in Fig. 3. The solid curve is the theoretical prediction of the reciprocal susceptibility (per Ni) [4]. The change in slope, visible in the corresponding plots of all compounds reported here, is characteristic of linear trimers with an antiferromagnetic exchange interaction between nearest neighbours. From Table VI, it is clear that the Ni trimers show a very similar magnetic behaviour, that seems to be independent of the crystal packing (no isomorphism was observed between compounds containing different ligands, *vide supra*). However, in case of $\text{Ni}_3(\text{adetr})_4\text{F}_2(\text{NCS})_4(\text{H}_2\text{O})_2$, no fit could be obtained down to 4 K, because μ_{eff} increases at temperatures below 26 K. This phenomenon might be due to the presence of a monomeric impurity. Unfortunately, interpretation of the magnetic data of the Co trimers appears to be far more difficult, as a result of appreciable g -factor anisotropy and the effective spin 1/2 approximation at lower temperatures. Therefore, an Ising Hamiltonian was used for the data interpretation [39]:

$$\mathcal{H} = -2J(S_{1z}S_{2z} + S_{2z}S_{3z}) - 2J_{13}S_{1z}S_{3z} + g\mu_B H_x(S_{1z} + S_{2z} + S_{3z})$$

where $J=J_{12}=J_{23}$ (J_{13} was again taken as zero). The susceptibility data were fitted to the expression [4]:

$$\chi = \frac{N_A g_{\parallel}^2 \mu_B^2}{36kT} \frac{[2 + e^{-x} + 9e^x]}{[2 + e^{-x} + e^x]}$$

($x = J/kT$, spin 1/2 approximation, χ_{\perp} is neglected)

Figure 4 shows the reciprocal susceptibility vs. temperature plot of $[\text{Co}_3(\text{tmtr})_4\text{F}_2(\text{NCS})_4(\text{H}_2\text{O})_2](\text{H}_2\text{O})_4$; the solid curve is the theoretical prediction of the reciprocal susceptibility based on the Ising

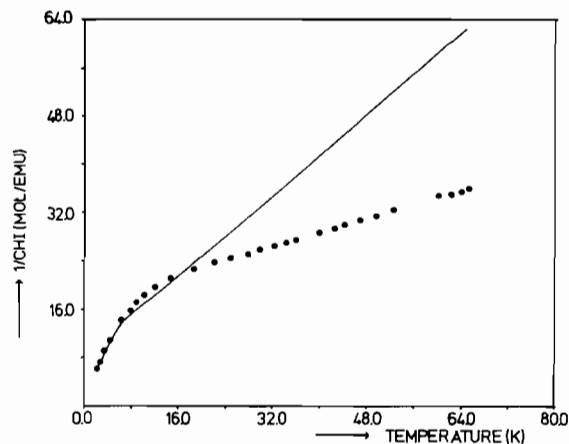


Fig. 4. Plot of the reciprocal magnetic susceptibility ($1/\chi$) vs. temperature of $[\text{Co}_3(\text{tmtr})_4\text{F}_2(\text{NCS})_4(\text{H}_2\text{O})_2](\text{H}_2\text{O})_4$. The drawn curve is the theoretical prediction of $1/\chi$ for a linear Ising trimer with $g_{\parallel}=6.1(1)$ and $J_{\parallel}=-7(1)$ cm^{-1} , assuming an effective spin of 1/2 for Co (diamagnetic correction = -175×10^{-6} e.m.u. per Co).

Hamiltonian given above. Figure 4 is representative for the series of Co trimers in the sense that it shows that the magnetic data do not fit satisfactorily to the equation given above. The fitting problems might be caused by the neglect of χ_{\perp} or by a breakdown of the spin 1/2 approach at higher temperatures. However, a more likely cause is an inappropriate choice of the Hamiltonian; the Ising Hamiltonian given above is only correct if the g -tensors of the central and terminal Co ions are collinear. The difference in the coordination spheres of the individual Co ions and the distortion of the octahedra of the terminal metal ions suggest that this condition might not be fulfilled. Therefore, for a more detailed study, single-crystal measurements are needed. Theoretical curves of g_{\perp} vs. g_{\parallel} for Co in trigonal and tetragonal ligand fields in the weak-field and strong-field approximations were described by Abragam and Price [40] and by Griffith [41]. These curves show that g_{\parallel} can have a maximum value of 9. The abnormal g_{\parallel} value of 9.21 observed for $\text{Co}_3(\text{adetr})_4\text{F}_2(\text{NCS})_4(\text{H}_2\text{O})_2$ probably results from the neglect of susceptibility data below 16 K; μ_{eff} increases at lower temperatures, as is the case in the corresponding Ni trimer. Table VI clearly illustrates the sensitivity of the g values to small changes in the geometry around the Co(II) ion, which was already pointed out by Abragam and Price [40].

Recently, structurally closely-related linear trimers were reported containing end-on thiocyanate bridges in stead of bridging fluoride anions [14]. The exchange interactions observed in these NCS-bridged compounds appear to shift towards the ferromagnetic region, as is illustrated by a J -value of $+9.6(1)$ cm^{-1} observed for $\text{Ni}_3(\text{detrH})_6(\text{NCS})_6(\text{H}_2\text{O})_2$ (the

J -value for $\text{Ni}_3(\text{detrH})_6\text{F}_2(\text{NCS})_4(\text{H}_2\text{O})_2$ is $-11.1(9)$ cm^{-1} , see Table VI). It is, however, premature to conclude from these data that the main exchange pathway is via the bridging anion, not only because the metal-to-bridging triazole distances in the two compounds are different, but also because linear trimeric compounds containing triple 1,2-bidentate triazole bridges show J -values of the same order of magnitude as the compounds reported here, in spite of considerably larger (≈ 0.5 Å) $\text{M}\cdots\text{M}$ distances [21, 22]. For similar reasons, a comparison of the magnetic data of the compounds $\text{M}_3(\text{detrH})_6\text{F}_2(\text{NCS})_4(\text{H}_2\text{O})_2$ and $\text{M}_3\text{L}_4\text{F}_2(\text{NCS})_4(\text{H}_2\text{O})_x$ (reported here) is rather speculative; moreover, in the latter compounds, hydrogen-bonding interactions involving the fluoride anion (*vide supra*) are likely to affect the magnetic exchange interaction observed.

Concluding Remarks

The results described in the present paper show that fluoride anions are easily incorporated in trimeric Co and Ni compounds containing double 1,2-bidentate substituted 1,2,4-triazole bridges between the metal ions. All eight compounds reported show a weak antiferromagnetic exchange interaction between neighbouring metal ions; the magnetic behaviour of the Ni trimers is very similar and relatively independent of the crystal packing. Interpretation of the magnetic data of the Co trimers is far less straightforward than for the Ni analogues, and single-crystal measurements are needed to obtain information about the g -tensors of the individual Co ions.

Supplementary Material

The additional material described herein is available from the authors on request.

Acknowledgements

The authors are indebted to Drs. J. Jordanov (Centre d'Etudes Nucléaires de Grenoble, France) and C. J. O'Connor (University of New Orleans, U.S.A.) for carrying out some of the magnetic susceptibility measurements, and to Dr. W. Hinrichs for performing the X-ray data collection. We are also grateful to Dr. R. A. G. de Graaff for his interest in this study. The investigation was supported by the Netherlands Foundation for Chemical Research (SON) with financial aid from the Netherlands Organisation for the Advancement of Pure Research (ZWO).

References

- 1 J. Reedijk and R. W. M. ten Hoedt, *Recl. Trav. Chim. Pays-Bas*, **101**, 49 (1982).
- 2 J. Reedijk, *Comm. Inorg. Chem.*, **1**, 379 (1982).
- 3 F. J. Rietmeijer, R. A. G. de Graaff and J. Reedijk, *Inorg. Chem.*, **23**, 151 (1984).
- 4 F. J. Rietmeijer, G. A. van Albada, R. A. G. de Graaff, J. G. Haasnoot and J. Reedijk, *Inorg. Chem.*, **24**, 3597 (1985).
- 5 W. C. Velthuizen, J. G. Haasnoot, A. J. Kinneking, F. J. Rietmeijer and J. Reedijk, *J. Chem. Soc., Chem. Commun.*, 1366 (1983).
- 6 M. F. Charlot, S. Jeannin, Y. Jeannin, O. Kahn, J. Lucresse-Abaul and J. M. Frere, *Inorg. Chem.*, **18**, 1675 (1979).
- 7 V. H. Crawford, H. W. Richardson, J. R. Wasson, D. J. Hodgson and W. E. Hatfield, *Inorg. Chem.*, **15**, 2107 (1976).
- 8 P. J. Hay, J. C. Thibeault and R. Hoffmann, *J. Am. Chem. Soc.*, **97**, 4884 (1975) and refs. therein.
- 9 O. Kahn, *Inorg. Chim. Acta*, **62**, 1 (1982).
- 10 W. E. Marsh, W. E. Hatfield and D. J. Hodgson, *Inorg. Chem.*, **21**, 2679 (1982).
- 11 W. E. Marsh, T. L. Bowman, C. S. Harris, W. E. Hatfield and D. J. Hodgson, *Inorg. Chem.*, **20**, 3864 (1981).
- 12 W. E. Marsh, K. C. Patel, W. E. Hatfield and D. J. Hodgson, *Inorg. Chem.*, **22**, 511 (1983) and refs. therein.
- 13 S. Sikorav, I. Bkouche-Waksman and O. Kahn, *Inorg. Chem.*, **23**, 490 (1984) and refs. therein.
- 14 G. A. van Albada, R. A. G. de Graaff, J. G. Haasnoot and J. Reedijk, *Inorg. Chem.*, **23**, 1404 (1984).
- 15 R. Stollé, *Ber. Dtsch. Chem. Ges.*, **32**, 797 (1899).
- 16 G. F. Duffin, *J. Chem. Soc.*, 3799 (1959).
- 17 'International Tables for X-ray Crystallography, Vol. IV', Kynoch Press, Birmingham, 1974.
- 18 A. J. Kinneking and R. A. G. de Graaff, *J. Appl. Crystallogr.*, **17**, 364 (1984).
- 19 J. Reedijk, W. L. Driessen and W. L. Groeneveld, *Recl. Trav. Chim. Pays-Bas*, **88**, 1095 (1969).
- 20 J. Reedijk, P. W. N. M. van Leeuwen and W. L. Groeneveld, *Recl. Trav. Chim. Pays-Bas*, **87**, 129 (1968).
- 21 L. R. Groeneveld, G. Vos, R. A. le Febre, R. A. G. de Graaff and J. G. Haasnoot, *Inorg. Chim. Acta*, **102**, 69 (1985).
- 22 G. Vos, J. G. Haasnoot, P. L. M. Schaminee, G. C. Verschoor and J. Reedijk, *Inorg. Chim. Acta*, **105**, 31 (1985).
- 23 P. C. H. Mitchell and R. J. P. Williams, *J. Chem. Soc.*, 1912 (1960).
- 24 M. Kabesova and J. Gazo, *Chem. Zvesti*, **34**, 800 (1980).
- 25 R. J. H. Clark and C. S. Williams, *Spectrochim. Acta*, **22**, 1081 (1961).
- 26 H. Carbacho, B. Ungerer and G. Contreras, *J. Inorg. Nucl. Chem.*, **32**, 579 (1970).
- 27 R. A. Bailey, S. L. Kozak, T. W. Michelsen and W. N. Mills, *Coord. Chem. Rev.*, **6**, 407 (1971).
- 28 J. Chat and L. A. Duncanson, *Nature (London)*, **178**, 997 (1956).
- 29 J. Chat, L. A. Duncanson, F. A. Hart and P. G. Owston, *Nature (London)*, **181**, 43 (1958).
- 30 M. M. Chamberlain and J. C. Bailor Jr., *J. Am. Chem. Soc.*, **81**, 6412 (1959).
- 31 M. E. Baldwin, *J. Chem. Soc.*, 471 (1961).
- 32 J. Lewis, R. S. Nyholm and P. W. Smith, *J. Chem. Soc.*, 4590 (1961).
- 33 A. Sabatini and I. Bertini, *Inorg. Chem.*, **4**, 959 (1965).
- 34 G. J. Long, D. Lindner, R. L. Lindvedt and J. W. Guthrie, *Inorg. Chem.*, **21**, 1431 (1982).
- 35 A. P. Ginsberg, R. L. Martin and R. C. Sherwood, *Inorg. Chem.*, **7**, 932 (1968).

- 36 P. D. W. Boyd and R. L. Martin, *J. Chem. Soc., Dalton Trans.*, 92 (1979).
- 37 D. J. Mackey and R. L. Martin, *J. Chem. Soc., Dalton Trans.*, 702 (1978).
- 38 G. Vos, A. J. de Kok and G. C. Verschoor, *Z. Naturforsch., Teil B*, 368, 809 (1981).
- 39 J. C. Bonner, H. Kobayashi, I. Tsujikawa, Y. Nakamura and S. A. Friedberg, *J. Chem. Phys.*, 63, 19 (1975).
- 40 A. Abragam and M. H. L. Price, *Proc. R. Soc. London, Ser. A*, 206, 173 (1951).
- 41 J. S. Griffith, 'The Theory of Transition-Metal Ions', Cambridge University Press, Cambridge, 1971.